

**SINGULAR INTEGRAL METHOD FOR THE
PULSE-MODULATED MICROWAVE ELECTRIC FIELD
COMPUTATIONS IN A 3D HEART MODEL**

L. Nickelson and S. Asmontas

Semiconductor Physics Institute
A. Gostauto str. 11, LTC01108 Vilnius, Lithuania

R. Martavicius

Electronic Systems Department
Electronics Faculty
Vilnius Gediminas Technical University
Naugarduko str. 41, LT-03227 Vilnius, Lithuania

V. Engelson

Linköping University
SE-58183, Linköping, Sweden

Abstract—The electrodynamic rigorous solution of Maxwell's equations related to the microwave pulse propagation inside a three-dimension heart model is presented here. The boundary problem was solved by using the singular integral equations' method. The carrier microwave frequency is 2.45 GHz. The pulse durations were always equal to 20 ms. The modulating signals are triangular video pulses with the on-off time ratio equal to 5 and 100. The model heart was limited by a non-coordinate shape surface and it consisted of two different size cavities. The heart cavities were schematic images of the left and right atriums and ventricles. In our calculations the cavities were filled with blood with the permittivity $\varepsilon_2 = 58 - i19$ and the walls of the heart consisted of myocardium tissue with the permittivity $\varepsilon_1 = 55 - i17$. Microwave electric field distributions were analysed at four longitudinal cross-sections of the heart model.

1. INTRODUCTION

In the last years investigations of the medical effects on the influence of microwave radiations on biological human organs have greatly increased. The main reason for the increased interest is because of the huge amount of man-made microwave fields in the environment around people. Scientific papers analyze microwave problems in diverse ways but most of them are devoted to experimental investigations only. These investigations are carried out by dosimeters and spectroscopy issues on cultured cells, isolated organs, animals and humans. The influence of microwaves on living organisms can produce positive and negative phenomena [1–4]. In references [3–7] microwave exposure can stimulate tissue repair, regeneration, relieved stress and facilitated recovery in animals and humans. It is important to research these phenomena which are dependent on frequencies, waveforms, amplitudes of microwaves and other parameters. The biological interaction of pulse-modulated electromagnetic fields and protection of humans from fields emitted from radars is analysed in [8]. Solution of electromagnetic scattering field problems are very actual nowadays problems [9–16].

In this present article our numerical investigations are devoted to the influence of the microwave pulses on a three-dimensional (3D) heart model, when the modulating signal is a triangular video pulse. In our previous articles [17, 18] we analyzed the scattered electric field on the 3D heart model. The heart model was illuminated by an incident vertically and horizontally polarized plane microwave from an external point source. In our articles [19–22] we analyzed the microwave electric field distribution of a 3D heart model depending on the shape and location of a microwave catheter which was placed inside of the model. In [23] we presented our investigations of the microwave electric field distributions into a heart model when the modulating signal of microwaves was a rectangular video pulse.

2. SIE METHOD FOR MICROWAVE FIELDS ANALYSES

We formulated our electro-dynamical problem like this: an antenna radiates a microwave pulse into a 3D heart model (Fig. 1). The heart model has an intricate shape. An antenna is placed outside the heart model touching it. We assumed the monochromatic carrier microwave with an angular frequency $\omega_0 = 2\pi f_0$ was modulated with a triangular video pulse. Mathematically we presented the monochromatic carrier microwave with a harmonic cosine function $\cos(\omega_0 t)$.

We calculated for two values of the on-off time ratio T/τ .

The pulse durations τ were always equal to a constant magnitude. Magnitudes of the pulse period T were different in our calculations. In this article we presented the algorithm that is based on the singular integral equations (SIE) method, which allowed us to carry out numerical investigations of an electric field distribution into a 3D heart model (Fig. 1). The surface of the 3D heart model as well the antenna was created in the 3D Studio MAX. This tool exports the surfaces as a set of triangles with a normal vector on certain surface points. The heart model consisted of cardiac muscle regions and the right and left atriums with ventricles cavities which were filled with blood. The width a of this model was 9 cm, the length b was 13 cm, distance $d = 9$ cm, the thickness of the model is 8 cm. Here we assumed that the antenna was made of ideal metal and radiated a microwave pulse. We also assumed that a microwave point source was placed at the tip of the antenna. The center of the coordinate system and the microwave point source placed in the middle of the model's thickness. The coordinates of the point source are $(0, 0, 9)$. To present the field in integral form for this electro-dynamical problem we used the solution to the Maxwell's equations with electric and magnetic point sources: $\text{rot}\vec{H} = i\omega\varepsilon_0\varepsilon\vec{E} + \vec{j}_e$; $\text{rot}\vec{E} = -i\omega\mu_0\mu\vec{H} - \vec{j}_m$. The solution to Maxwell's equations is constructed as a superposition of hybrid quasi-E and quasi-H waves. In our SIE method we separated the solution of equations from satisfying the boundary conditions [24].

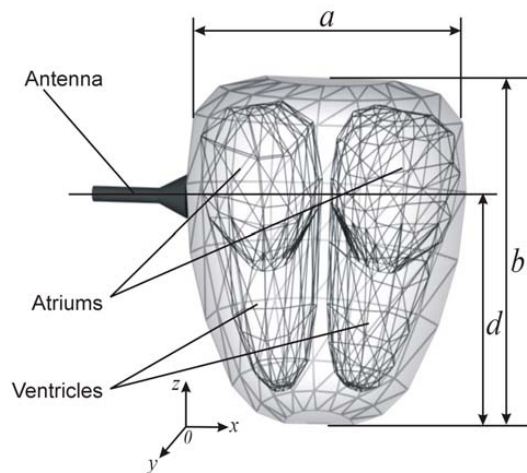


Figure 1. The heart model with the myocardium, the left and right atriums and ventricles used in computations.

In the beginning we found the solution of the differential equations having a δ -function on the right side, i.e., the solution to the point source problem. Then this fundamental solution is used in the integral representation of an electromagnetic field for solving an electrodynamic problem of an arbitrarily shaped 3D body, which can be characterized by a set of the complex dielectric permittivities. The electric field representation is [24]:

$$\vec{E}(\vec{r}_1) = \int_{S_i} \mu_e(\vec{r}_0) \left[\frac{1}{\chi} \psi_1 + \vec{n}(\vec{r}_0) \right] \beta_0 dS - iZ_0 \sqrt{\frac{\mu_p}{\varepsilon_p}} \int_{S_i} \mu_h(\vec{r}_0) \psi_2 \beta_1 dS; \quad (1)$$

$$\vec{H}(\vec{r}_1) = \frac{i}{Z_0} \sqrt{\frac{\varepsilon_p}{\mu_p}} \int_{S_i} \mu_h(\vec{r}_0) \psi_2 \beta_1 dS + \int_{S_i} \mu_e(\vec{r}_0) \left[\frac{1}{\chi} \psi_1 + \vec{n}(\vec{r}_0) \right] \beta_0 dS. \quad (2)$$

Here unknown functions $\mu_e(\vec{r}_0)$ and $\mu_h(\vec{r}_0)$ respectively are electric and magnetic source densities at the point \vec{r}_0 on the surface of the 3D heart model. The quantity $\vec{n}(\vec{r}_0)$ is a unit normal vector to the surface at the same point. The quantity $\vec{n}(\vec{r}_1)$ is a unit normal vector to the surface at the point \vec{r}_1 where we determinate the fields $\vec{E}(\vec{r}_1)$ and $\vec{H}(\vec{r}_1)$. The magnitude $\beta_0 = h_0 \left(k \sqrt{\varepsilon_p \mu_p} |\vec{r}_1 - \vec{r}_0| \right)$ is the spherical Hankel function of the zeroth order and the second kind and $\beta_1 = h_1 \left(k \sqrt{\varepsilon_p \mu_p} |\vec{r}_1 - \vec{r}_0| \right)$ is the spherical Hankel function of the first order and the second kind. The quantity $|\vec{r}_1 - \vec{r}_0|$ is the distance from the point \vec{r}_1 where we want to determinate the fields $\vec{E}(\vec{r}_1)$ and $\vec{H}(\vec{r}_1)$ to the point \vec{r}_0 . The magnitude k is the wave number in free space and $Z_0 = \sqrt{\mu_0/\varepsilon_0}$ is the characteristic impedance of the free space. We assumed in this article that the complex permittivities $\varepsilon_p = \varepsilon'_p - i\varepsilon''_p$ and permeabilities μ_p of the heart tissue and the surrounding areas are scalars, where indexes $p = 1, 2, 3$ represent the cardiac muscle, the blood and free space respectively. The magnitude $\nabla = \hat{i} \frac{\partial}{\partial x} + \hat{j} \frac{\partial}{\partial y} + \hat{k} \frac{\partial}{\partial z}$ is the gradient operator. The magnitude $\psi_1 = \nabla(\vec{n}(\vec{r}_0), \nabla)$ is the gradient of a dot product of the vector $\vec{n}(\vec{r}_0)$ and the vector operator ∇ . The magnitude $\psi_2 = \left[\vec{n}(\vec{r}_0), \frac{\vec{r}_1 - \vec{r}_0}{|\vec{r}_1 - \vec{r}_0|} \right]$ is a cross product of two vectors. Here we will write the boundary conditions only for electric field components on the external heart surface. The external surface S_3 divides the area into two parts described by the values ε_3, μ_3 (for air, in the next expressions the top index is “-”) and ε_1, μ_1 (for myocardium, in the next expressions the top index is “+”). To satisfy the boundary conditions for the electric field components we equating

the vector product $[\vec{n}(\vec{r}_1), \vec{E}(\vec{r}_1)]^+ = [\vec{n}(\vec{r}_1), \vec{E}(\vec{r}_1)]^-$. We arrive at the integral equation for the surface densities $\mu_e^+(\vec{r}_0)$, $\mu_e^-(\vec{r}_0)$ and $\mu_h^+(\vec{r}_0)$, $\mu_h^-(\vec{r}_0)$:

$$\begin{aligned}
 & \int_{S_i} \mu_e^+(\vec{r}_0) \left[\psi_3 \psi_6 \left(\frac{3\beta_1}{\sqrt{\chi} |\vec{r}_1 - \vec{r}_0|} - \beta_0 \right) + \psi_7 \left(\beta_0 - \frac{\beta_1}{\sqrt{\chi} |\vec{r}_1 - \vec{r}_0|} \right) \right] dS \\
 & - \left(iZ_0 \int_{S_i} \mu_h^+(\vec{r}_0) n(\vec{r}_0) \psi_4 - \frac{\vec{r}_1 - \vec{r}_0}{|\vec{r}_1 - \vec{r}_0|} \psi_5 \beta_1 \right) dS \\
 = & [\vec{n}(\vec{r}_1), \vec{E}_{mw}(t, \vec{r}_1)]^- + \int_{S_i} \mu_e^-(\vec{r}_0) \left[\psi_3 \psi_6 \left(\frac{3\beta_1}{\sqrt{\chi} |\vec{r}_1 - \vec{r}_0|} - \beta_0 \right) \right. \\
 & \left. + \psi_7 \left(\beta_0 - \frac{\beta_1}{\sqrt{\chi} |\vec{r}_1 - \vec{r}_0|} \right) \right] dS \\
 & + \left(iZ_0 \int_{S_i} \mu_h^-(\vec{r}_0) n(\vec{r}_0) \psi_4 - \frac{\vec{r}_1 - \vec{r}_0}{|\vec{r}_1 - \vec{r}_0|} \psi_5 \beta_1 \right) dS, \quad (3)
 \end{aligned}$$

where magnitudes $\psi_3 = \left(\vec{n}(\vec{r}_0), \frac{\vec{r}_1 - \vec{r}_0}{|\vec{r}_1 - \vec{r}_0|} \right)$, $\psi_4 = \left(\vec{n}(\vec{r}_1), \frac{\vec{r}_1 - \vec{r}_0}{|\vec{r}_1 - \vec{r}_0|} \right)$, $\psi_5 = \left(\vec{n}(\vec{r}_1), \vec{n}(\vec{r}_0) \right)$ are the scalar product of two vectors and magnitudes $\psi_6 = \left[\vec{n}(\vec{r}_1), \frac{\vec{r}_1 - \vec{r}_0}{|\vec{r}_1 - \vec{r}_0|} \right]$, $\psi_7 = [\vec{n}(\vec{r}_1), \vec{n}(\vec{r}_0)]$ are the vector product of two vectors.

Equating the vector product $[\vec{n}(\vec{r}_1), \vec{H}(\vec{r}_1)]^+ = [\vec{n}(\vec{r}_1), \vec{H}(\vec{r}_1)]^-$ for the magnetic field we received a similar integral equation as (3) for the magnetic field. The vector $\vec{E}_{mw}(t, \vec{r}_1)$ in the equation (3) is the electric field of the microwave pulse that is radiated by an antenna (Fig. 1). We assumed that the magnitude of this vector $\vec{E}_{mw}(t, \vec{r}_1)$ when the carrier microwave is modulated by triangular video pulses [25] is equal to:

$$\vec{E}_{mw\Delta}(t, \vec{r}_1) = \frac{E_0}{2q} \left\{ 1 + 2 \sum_{k=1}^{2q} \left[\frac{\sin(k\pi/2q)}{k\pi/2q} \right]^2 \cos(k\omega_1 t) \right\} \cos(\omega_0 t), \quad (4)$$

where $\omega_1 = 2\pi/T$, the triangular video pulse on-off time ratio is $q = T/\tau$.

The components (harmonics) of the amplitude spectrum of the periodic sequence of the triangular video pulses are equidistantly

located on the axis of frequencies with the interval $f_1 = 1/T$. The width of the spectrum of periodic triangular video pulses is the value of the inversely proportional pulse duration $F = 2/\tau$ and does not depend on the period the pulse period T . Since the period of the pulse period T is not very large in the comparison with the pulse duration τ , then for the triangular pulses it suffices to take a quantity of the spectrum components $K = 2q$. These spectrum components are located in the main spectrum lobe. The shape of the triangular impulses will be good enough in this case.

The system of SIE was reduced to an algebraic system of linear equations and this system was solved numerically. Our calculations were compared to experimental and theoretical results for simple diffraction problems from different articles. These comparisons are given in [17, 18] and [24]. We believe that we can use our SIE method to study electromagnetic processes in a heart model which is under the influence some microwave pulses.

3. NUMERICAL RESULTS

In our calculations the frequency of the carrier microwave was $f_0 = 2.45$ GHz. The magnitude of the real and imaginary parts of the permittivity of the cardiac muscle is $\varepsilon_1 = 55 - i17$ and the blood is $\varepsilon_2 = 58 - i19$.

Figures 2 and 3 show the distribution of the normalized electric field modulus $|\vec{E}|/|\vec{E}_{\max}|$ at the longitudinal cross-section along the z coordinate axis. Here the magnitude \vec{E}_{\max} is the amplitude of the microwave electric field in the center of the antenna tip and the electric field $|\vec{E}| = \sqrt{E_x^2 + E_y^2 + E_z^2}$. The microwave pulse that is radiated by an antenna (Fig. 1) is obtained when the monochromatic carrier microwave signal with frequency f_0 is modulated by the triangular video pulses with certain parameters τ and T .

In our calculation a video pulse is formed of spectrum components (harmonics). In all investigated cases the width of spectrum of periodic triangular video pulses is equal to $F = 100$ Hz. We operate in the range of frequencies $f_0 \pm F = (2.45 \cdot 10^9 \pm 100)$ Hz. So the complex permittivities of the cardiac muscle and the blood are constant at this frequency range.

In Figures 2 and 3 we see the electric field distribution when the monochromatic carrier microwave was modulated by the triangular video pulses with a different on-off time ratio T/τ , when $\tau = 20$ ms.

Figures 2 and 3 show the distributions in four heart model cross-sections which are removed from the antenna tip by the distance 0.3 cm,

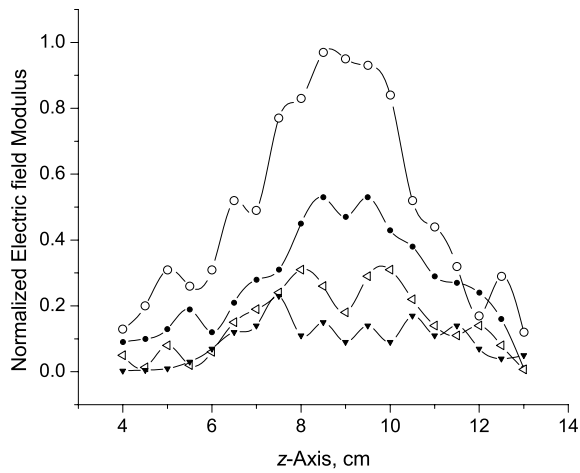


Figure 2. Distribution of magnitude $|\vec{E}|/|\vec{E}_{\max}|$ along the z axis in four transversal cross sections with the coordinate $x = 0.3$ cm (curve with circles), 3 cm (curve with black dots), 5 cm (curve with hollow triangles), 7 cm (curve with black triangles) when a modulating signal is a triangular video pulse with the on-off time ratio $T/\tau = 5$.

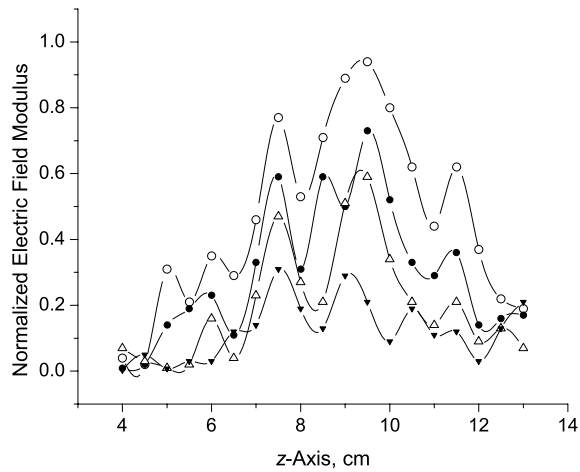


Figure 3. Distribution of magnitude $|\vec{E}|/|\vec{E}_{\max}|$ along the z axis in three transversal cross sections with the coordinate $x = 0.3$ cm (curve with circles), 3 cm (curve with black dots), 5 cm (curve with hollow triangles), 7 cm (curve with black triangles) when a modulating signal is a triangular video pulse with the on-off time ratio $T/\tau = 100$.

3 cm, 5 cm and 7 cm. As it was mentioned the source of the microwave pulses is placed in the point with the coordinate $z = 9$ (cm). We assume that this point is a central point when we examine curves on the graphs.

Curve with the circles shows the electric field distribution at the nearest cross section to the antenna tip. We see that the electric field amplitude is the largest in this first cross-section of the heart almost in all points. So the closer a cross-section to the antenna tip the larger usually is the amplitude of the electric field in that cross section. We see that at the points which are removed from the antenna tip the opposite dependences in distributions of the electric field amplitude can be observed.

The distribution of the normalized electric field amplitudes when a pulse period T equal to 100 ms is shown in Figure 2. We see interference pictures of the ten spectrum components in the four heart cross-sections. Here the microwave electric field amplitude changes slightly asymmetrically to the antenna tip when the microwave pulses propagate into the heart model. It happened because the chambers of the heart model from which surfaces reflected the microwave pulse are located slightly asymmetrically with respect to the antenna tip. We see the microwave electric field distributions into the heart model cross-sections undergo some distortions.

We see that the maximum of the normalized electric field amplitudes for the curve when the distance $x = 0.3$ cm is a little bit shifted from the central point to the left. There are clearly expressed minimums of the normalized electric field amplitudes in the central point for curves when the distances x equal to 3 cm, 5 cm and 7 cm.

The basic tendency all curves in Figure 2 is that the strongest electric field concentrates in an area around the central point with a radius about two centimeters and in the center of this area may be a minimum. The interference extremes are expressed weakly in Figure 2.

The distribution of the normalized electric field amplitudes when a pulse period T equal to 2 s is shown in Figure 3. Here the on-off time ratio is $T/\tau = 100$ and the number of spectrum components K is two hundred. The picture of the interference of two hundred spectrum components has the several sharp resonant extremums along the z -axis. We see that the largest electric field maximums for all curves are shifted to the right from the central point. There are strong enough lateral maximums closely to the main maximum.

Analysing Figures 2 and 3 we see that the distributions of the microwave electric field inside of the heart model are stipulated by the phenomena of the microwave pulse propagation inside of an inhomogeneous media which has a complicated shape. It is

important to note several factors which determine the microwave pulse propagation: 1) the modulating signal which is a video pulse we describe by formula (4) as a sum of spectrum components (harmonics); 2) a number of harmonics which approximate the modulating video pulse is chosen proportional to the on-off time ratio of the pulse in order to the shape of triangular pulse would be good; 3) a number of spectrum components depends on the form of a video pulse also; 4) spectrum components of the microwave signals can reflect repeatedly from the interior and external heart model surfaces; 5) the interference of spectrum components occurs inside of the heart model; 6) the media of the heart model is the cardiac muscle and blood which are the lossy materials with complex dielectric permittivities which have large imaginary parts and therefore a microwave signal can be attenuated.

Analysing Figures 2 and 3 we see also that the penetration into lossy medium of the pulse-modulated microwave is deeper the compare with the unmodulated microwave. Penetration depths into the cardiac muscle and blood are 1.6 cm and 1.8 cm at the frequency 2.45 GHz. We see in Figures 2 and 3 that the penetration of the pulse-modulated microwave into the heart model is approximately two or three times larger in the comparison with the unmodulated microwave.

The authors of references [4–7] prove that the influence of modulated microwave signals on different biological systems exists. Article [26] explains this phenomenon. In order to the modulated microwave signals would influence on a living organism it is necessary to demodulate this signal and for this reason it is necessary to use a non-linear element. But in biology the cell membrane fulfills the function of a non-linear element [26]. So the microwave pulse phenomenon makes it possible to create advanced microwave devices.

4. CONCLUSION

1. We used our SIE method to solve Maxwell's equations relating to the propagation of microwave pulses inside of a 3D heart model consisting of very lossy media.
2. We investigated microwave electric field distributions at several cross-sections of a 3D heart model. We found that the microwave electric field distribution depends on the on-off time ratio of modulating video pulses when their on-off time ratio magnitudes differ in twenty times.
3. We found that the amplitude of the electric field decreased in different way dependent on the direction while the microwave pulses were moving away from the antenna tip. This happened because the 3D heart model consists of different lossy materials which were described

by complex dielectric permittivities and the heart boundary surfaces have intricate shape.

REFERENCES

1. Rosen, A., A. J. Greenspon, and P. Walinsky, "Microwaves treat heart disease," *IEEE Microwave Magazine*, Vol. 8, No 1, 70–75, 2007.
2. Barker, A. T., P. R. Jackson, H. Rarry, L. A. Coulton, G. G. Cook, and S. M. Wood, "The effect of GSM and TETRA mobile handset signals on blood pressure, catechol levels and heart rate variability," *Bioelectromagnetics*, Vol. 28, No. 6, 433–438, 2007.
3. Moore, S. K., "Electronic implants and electromagnetic pulses," *IEEE Spectrum*, Vol. 43, No. 3, 19–25, 2006.
4. Sanders, A. P., W. T. Joines, and J. W. Allis, "Effects of continuous-wave, pulsed, and sinusoidal-amplitude-modulated microwaves on brain energy metabolism," *Bioelectromagnetics*, Vol. 6, No. 1, 89–97, 1985.
5. Huber, R., V. Treyer, J. Schuderer, T. Berthold, A. Buck, N. Kuster, H. P. Landolt, and P. Achermann, "Exposure to pulse-modulated radio frequency electromagnetic fields affects regional cerebral blood flow," *European Journal of Neuroscience*, Vol. 21, No. 4, 1000–1006, 2005.
6. Maier, R., S. E. Greter, and N. Maier, "Effects of pulsed electromagnetic fields on cognitive processes — A pilot study on pulsed field interference with cognitive regeneration," *Acta Neurologica Scandinavica*, Vol. 110, No. 1, 46–52, 2004.
7. Beason, R. C. and P. Semm, "Responses of neurons to an amplitude modulated microwave stimulus," *Neuroscience Letters Elsevier*, Vol. 333, No. 3, 175–178, 2002.
8. Kubacki, R., "Biological interaction of pulse-modulated electromagnetic fields and protection of humans from exposure to fields emitted from radars," *Proceedings of 17th International Conference on Microwaves, Radar and Wireless Communications, MIKON-2008*, Vol. 2, 360–366, Wroclaw, Poland, May 19–21, 2008.
9. Ahmed, S. and Q. A. Naqvi, "Electromagnetic scattering from parallel perfect electromagnetic conductor cylinders of circular cross-sections using an iterative procedure," *J. of Electromagnetic Waves and Applications*, Vol. 22, No. 7, 987–1003, 2008.
10. Ozgun, O. and M. Kuzuoglu, "Finite element analysis of electromagnetic scattering problems via iterative leap-field domain

- decomposition method,” *J. of Electromagnetic Waves and Applications*, Vol. 22, No. 2–3, 251–266, 2008.
11. Liu, X., B. Z. Wang, and S. Lai, “Element-free Galerkin method in electromagnetic scattering field computation,” *J. of Electromagnetic Waves and Applications*, Vol. 21, No. 14, 1915–1923, 2007.
 12. Liu, Y., Z. Liang, and Z. Yang, “Computation of electromagnetic dosimetry for human body using parallel FDTD algorithm combined with interpolation technique,” *Progress In Electromagnetics Research*, PIER 82, 95–107, 2008.
 13. Zhang, H., S. Y. Tan, H. S. Tan, “A novel method for microwave breast cancer detection,” *Progress In Electromagnetics Research*, PIER 83, 413–434, 2008.
 14. Ho, M., F.-S. Lai, S.-W. Tan, and P.-W. Chen, “Numerical simulation of propagation of EM pulse through Lossless non-uniform dielectric slab using characteristic-based method,” *Progress In Electromagnetics Research*, PIER 81, 197–212, 2008.
 15. Ho, M. and F. S Lai,, “Effects of medium conductivity on electromagnetic pulse propagation onto dielectric half space: one-dimensional simulation using characteristic-based method,” *J. of Electromagnetic Waves and Applications*, Vol. 21, No. 13, 1773–1785, 2007.
 16. Abd-El-Raouf, H. E. and R. Mittra, “Scattering analysis of dielectric coated cones,” *J. of Electromagnetic Waves and Applications*, Vol. 21, No. 13, 1857–1871, 2007.
 17. Knisevskaja (Nickelson), L., V. Engelson, and K.-F. Berggren, “Singular integral equations’ method for computations of the scattering characteristics of a model heart exposed to electromagnetic radiation,” *Applied Mathematics and Computation Elsevier*, Vol. 138, Nos. 2–3, 545–553, 2003.
 18. Knisevskaja (Nickelson), L., V. Engelson, and K.-F. Berggren, “Accurate numerical method for calculating the diffraction characteristics of a human heart model,” *Electronics and Electrical Engineering*, Vol. 43, No. 1, 13–16, Kaunas, Technologija, 2003.
 19. Nickelson, L., S. Asmontas, V. Engelson, B. A. Galwas, and M. Tamosiuniene, “The computation of electrical fields on a heart model with a microwave catheter,” *Conference Proceedings of 15th International Conference on Microwaves, Radar and Wireless Communications, MIKON-2004*, Vol. 3, 849–852, Warsaw, Poland, May 17–19, 2004.
 20. Nickelson, L., S. Asmontas, K. Pozela, and V. Engelson, “The electrical field distribution on a model heart when a microwave antenna is placed inside it,” *Proceedings of Progress*

- In Electromagnetics Research Symposium (PIERS2004)*, 265–268, Pisa, Italy, March 28–31, 2004.
21. Nickelson, L., S. Ašmontas, V. Mališauskas, R. Martavicius, and V. Engelson, “An electrodynamic analysis of a model heart,” *Electronics and Electrical Engineering*, Vol. 63, No. 7, 57–61, Kaunas, Technologija, 2005.
 22. Nickelson, L., S. Asmontas, V. Shugurov, R. Martavicius, and V. Malisauskas, “SIE method of analysing microwave fields of a 3D heart model,” *Journal of Electromagnetic Waves and Applications*, Vol. 20, No. 2, 193–206, 2006.
 23. Nickelson, L., S. Asmontas, R. Martavicius, V. Engelson, and D. Zylkov, “Microwave pulses propagation inside of a 3D heart model,” *Proceedings of 17th International Conference on Microwaves, Radar and Wireless Communications, MIKON-2008*, Vol. 3, 595–598, Wroclaw, Poland, May 19–21, 2008.
 24. Nickelson, L. and V. Shugurov, *Singular Integral Equations’ Methods for the Analysis of Microwave Structures*, 348, VSP Brill Academic Publishers, Leiden-Boston, 2005.
 25. Beleckij, A. J., V. P. Babak, *The Determinate Signals and Spectrums*, 502, “Kit” Publishers, Kiev, 2002 (in Russian).
 26. Haberland, L., “Why is a higher biological relevance attached to importance of pulsed signals?” *FGH-Newsletter*, No. 2, 18–21, 2005.